Mechanics of Materials 117 (2018) 32–40

Contents lists available at ScienceDirect

Mechanics of Materials

journal homepage: www.elsevier.com/locate/mechmat

Research paper

A pileup of edge dislocations against an inclined bimetallic interface

Vlado A. Lubarda

Department of NanoEngineering, University of California, San Diego; La Jolla, CA 92093-0448, USA

ARTICLE INFO

Keywords:
Back stress
Bimetallic interface
Dislocation
Pileup
Stress concentration

ABSTRACT

A pileup of edge dislocations against an arbitrarily inclined flat bimetallic interface is considered. Equilibrium positions of dislocations are determined for a given number of dislocations and specified material properties, assuming that the resolved shear stress along the pileup plane from a remotely applied loading is uniform and equal for all interface inclination angles. Numerical results are compared for pileups at 0°, 30°, 45°, and 60° relative to the interface normal. The overall dislocation distribution is mildly affected by the inclination of the interface, although there are some notable differences. While an inclined interface repels the first and last dislocation stronger than the orthogonal interface, for piled-up dislocations in-between this is not necessarily the case. Small differences in the pileup length and the proximity of the leading dislocation to differently inclined interfaces can considerably affect the interface stresses. The magnitude of interface stresses decreases with the increase of the shear moduli ratio G_2/G_1 due to stronger repulsion exerted on dislocations by stiffer interfaces. The disparity in Poisson's ratio also affects the interface stresses. The back stress behind a trailing dislocation is evaluated and discussed.

1. Introduction

The study of dislocation pileups against second-phase particles and grain boundaries has been a classical topic of mechanics and materials science of importance for the analysis of inelastic material response and fracture. An early study of dislocation pileups was performed by Eshelby et al. (1951), who considered pileups in an infinite homogeneous medium in which the leading dislocation was assumed to be locked. Further contributions were made by many investigators, who addressed pileups of screw and edge dislocations against circular inhomogeneities and bimetallic interfaces. The effects of elastic anisotropy and the nonlinearity due to dislocation cores were examined, as well as the stress fields of double ended pileups in stacked slip planes and of multiple dislocation-wall pileups (Chou, 1966; Barnett and Tetelman, 1967; Barnett, 1967; Kuang and Mura, 1968; Thölén, 1970; Smith, 1972; Kuan and Hirth, 1976; Wagoner, 1981; Öveçoğlu et al., 1987; Voskoboinikov et al., 2007; 2009; Hall, 2010; Baskaran et al., 2010; Geers et al., 2013; Scardia et al., 2014; Zhang, 2017; Kapoor and Verdhan, 2017).

Edge dislocation pileups against a plane bimetallic interface were studied analytically by the method of continuously distributed infinitesimal dislocations by Kuang and Mura (1968). They solved analytically the singular integral equation for equilibrium positions of dislocations, but their solution involved infinite products which were quite demanding for computations. Discrete edge dislocation pileups were investigated numerically by Kuan and Hirth (1976), who incorporated in their analysis the nonlinear dislocation core terms. Wagoner (1981) studied the corresponding anisotropic elastic effects. Öveçoğlu et al. (1987) also considered discrete edge dislocation pileups against a plane bimetallic interface, and evaluated the interface stresses for various combinations of material parameters. More recently, Voskoboinikov et al. (2009) presented an asymptotic analysis of dislocation pileups against a bimetallic interface, while Lubarda (2017a) presented an analysis of dislocation pileups against both a circular inhomogeneity and a flat bimetallic interface.

In all of the above work the dislocation pileups were assumed to be along the glide direction orthogonal to the interface. In the present paper we extend these analyzes by considering discrete edge dislocation pileups against a flat bimetallic interface which is arbitrarily oriented relative to the pileup (glide) direction. We solve numerically the nonlinear algebraic equations that specify equilibrium positions of dislocations, for a given number of dislocations and specified material properties. The magnitude of the resolved shear stress along the pileup direction is assumed to be uniform and equal for each inclination φ of the interface. The derivation of the expressions for dislocation forces, which must vanish in equilibrium, is lengthy and tedious, but we were able to cast them in a relatively compact form for any angle φ. The simplified expressions are then deduced for $\varphi = 0°$, 30°, 45°, and 60°. The overall dislocation distribution is mildly affected by the inclination of the interface, although there are some notable differences. While an inclined interface repels the first and last dislocation stronger than the interface orthogonal to the glide plane, for piled-up dislocations in-

E-mail address: vlubarda@ucsd.edu.

http://dx.doi.org/10.1016/j.mechmat.2017.10.010
Received 23 May 2017; Received in revised form 11 October 2017; Accepted 12 October 2017
Available online 16 October 2017

between this is not necessarily the case. Furthermore, small differences in the pileup length and the proximity of the leading dislocation to differently inclined interfaces can considerably affect the interface stresses. The magnitude of these stresses decreases with the increase of the shear moduli ratio G_2/G_1 due to stronger repulsion exerted on dislocations by stiffer interfaces. The disparity in Poisson's ratio also affects the interface stresses. The variation of the back stress behind a trailing dislocation of a pileup is determined for different orientation of the interface. There is a small effect of φ on the magnitude of the back stress. Far behind a trailing dislocation, the back stress approaches the stress levels caused by a superdislocation of the Burgers vector *Nb* located at the interface, independently of φ. An analysis of screw dislocation pileups against an inclined bimetallic interface is reported in Lubarda (2017b).

In the presented analysis, the dimensionless material parameters α and β (Dundurs, 1969) are used, which are defined in terms of $\Gamma = G_2/G_1$ and (ν_1, ν_2) by

$$\alpha = \frac{(1-\nu_1)\Gamma - (1-\nu_2)}{(1-\nu_1)\Gamma + (1-\nu_2)}, \quad 2\beta = \frac{(1-2\nu_1)\Gamma - (1-2\nu_2)}{(1-\nu_1)\Gamma + (1-\nu_2)}. \tag{1}$$

After nondimensionalisation of the problem, the two dimensionless parameters that play a prominent role for the most part of the analysis are the parameters q and γ, defined in terms of α and β by

$$q = \frac{\alpha-\beta}{1+\beta}, \quad g = \frac{(1+\alpha)\beta}{1-\beta^2}, \quad \gamma = q + g = \frac{\alpha+\beta^2}{1-\beta^2}. \tag{2}$$

For example, if $\Gamma = \infty$ (rigid interface, $G_2 > > G_1$), the dimensionless parameters are

$$\alpha = 1, \quad 2\beta = \frac{1-2\nu_1}{1-\nu_1}, \quad q = \frac{1}{3-4\nu_1}, \quad (1/3 \le q \le 1), \quad 2\gamma = q + \frac{1}{q}, \quad (1 \le \gamma \le 5/3).$$

If $\Gamma = 1$ (equal shear moduli of two materials, $G_1 = G_2$), then

$$\alpha = \beta = \frac{\nu_2 - \nu_1}{2 - (\nu_1 + \nu_2)}, \quad q = 0, \quad 2\gamma = \frac{\nu_2 - \nu_1}{1 - (\nu_1 + \nu_2)}.$$

2. Edge dislocation pileups

Fig. 1 shows a pileup of N positive edge dislocations of a Burgers vector $b_x = b > 0$ against a bimetallic interface inclined by an angle φ ≠ ± 90° relative to the glide plane normal. It is assumed that the resolved shear stress along the glide plane of dislocations, caused by remotely applied loading, is uniform along the glide plane and independent of φ. We denote this shear stress by τ^a. It is the only part of applied stress that is relevant to dislocation motion (glide) considered in this paper. The external loading has to be such that τ^a is directed toward the interface, i.e., $\tau^a_{xy}|_{y=0} = -\tau^a$, in order to have a driving force for piling-up of dislocations in the case $\Gamma > 1$. The contribution to the resolved shear stress from the interactions among dislocations in the presence of the interface can be calculated by using the results of Head (1953) and Dundurs (1969), as described in the appendix of the paper. For the ith dislocation, at the position x_i, this shear stress is

$$\tau^b(x_i) = k_1 b \frac{\gamma}{2x_i} + \sum_{j\neq i}^{N} \tau^{b,j}(x_i), \quad k_1 = \frac{G_1}{2\pi(1-\nu_1)}. \tag{3}$$

The first term on the right hand-side is the self-shear stress contribution of the dislocation at x_i, due to its image effects caused by the interface, while the second term is the sum of resolved shear stresses caused by all other dislocations in the pileup. In the equilibrium pileup configuration, the glide component of dislocation force on each dislocation must vanish,

$$f_i(x_i) = [\tau^b(x_i) - \tau^a]b = k_1 b^2 \frac{\gamma}{2x_i} + b\sum_{j\neq i}^{N} \tau^{b,j}(x_i) - \tau^a b = 0, \quad (i = 1, 2, 3, \cdots, N). \tag{4}$$

The expressions for $\tau^{b,j}(x_i)$ are derived in the appendix of this paper for any angle φ ≠ ± 90°. In particular, if the interface is orthogonal to glide plane ($\varphi = 0°$), the resolved shear stress $\tau^{b,j}(x_i)$ takes an explicit, compact form

$$\tau^{b,j}(x_i) = k_1 b\left[\frac{1}{x_i - x_j} + \gamma\frac{1}{x_i + x_j} + 2q\frac{x_j(x_i - x_j)}{(x_i + x_j)^3}\right]. \tag{5}$$

For $\varphi = 30°$, the expression is

$$\tau^{b,j}(x_i) = k_1 b\left[\frac{1}{x_i - x_j} + \frac{\gamma}{2}\frac{2x_i + x_j}{x_i^2 + x_j^2 + x_i x_j} + \frac{9q}{2}\frac{x_i x_j^2(x_i^2 - x_j^2)}{(x_i^2 + x_j^2 + x_i x_j)^3}\right], \tag{6}$$

while for $\varphi = 45°$,

$$\tau^{b,j}(x_i) = k_1 b\left[\frac{1}{x_i - x_j} + \gamma\frac{x_i}{x_i^2 + x_j^2} - q\frac{x_j(x_i^2 - x_j^2)(x_i^2 + x_j^2 - 4x_i x_j)}{(x_i^2 + x_j^2)^3}\right]. \tag{7}$$

Finally, for $\varphi = 60°$ the resolved shear stress is found to be

$$\tau^{b,j}(x_i) = k_1 b\left[\frac{1}{x_i - x_j} + \frac{\gamma}{2}\frac{2x_i - x_j}{x_i^2 + x_j^2 - x_i x_j} - \frac{q}{2}\frac{x_j(x_i^2 - x_j^2)(2x_i^2 + 2x_j^2 - 5x_i x_j)}{(x_i^2 + x_j^2 - x_i x_j)^3}\right]. \tag{8}$$

In the limiting case $\varphi = 90°$, a pileup is along the interface, made of N interface edge dislocations, provided that the leading dislocation in the pileup is locked. In this case, the interaction shear stress is

$$\tau^{b,j}(x_i) = (1+\gamma)k_1 b^2\left(\frac{1}{x_i} + \sum_{\substack{j=2\\ j\neq i}}^{N}\frac{1}{x_i - x_j}\right), \quad (i = 2, 3, \cdots N), \tag{9}$$

where x is measured from the position of the locked dislocation ($x_1 = 0$), and $1 + \gamma = (1+\alpha)/(1-\beta^2)$. From the physical point of view, pileups of interface dislocations are of less significance, albeit they may be of some interest in the analysis of semicoherent interfaces, for which interface dislocations play important role in misfit accommodation and strain relaxation (Freund, 1993; Lubarda and Kouris, 1996; Lubarda, 1998).

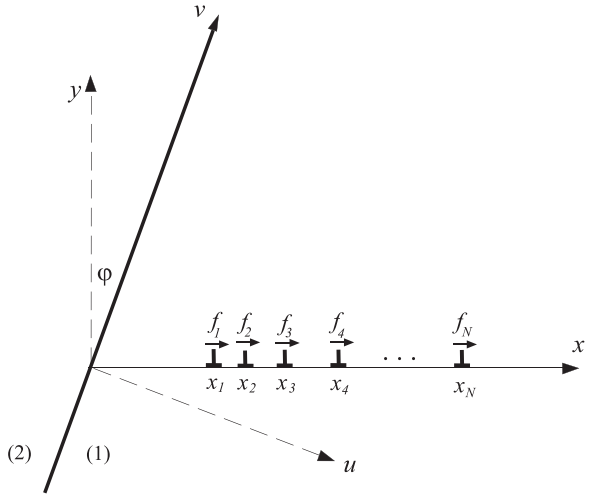

Fig. 1. A pileup of N edge dislocations against a bimetallic interface under uniform resolved shear stress along the glide plane $y = 0$. A bimetallic interface ($u = 0$) is inclined by an angle φ relative to the glide plane normal y. In the equilibrium configuration the configurational force on each dislocation vanishes ($f_i = 0$), which specifies the corresponding positions of dislocations x_i ($i = 1, 2, 3, \cdots, N$).

3. Equilibrium positions of dislocations

In the equilibrium configuration the dislocation force on each dislocation in a pileup must vanish ($f_i = 0$). In view of (4), this gives a system of N nonlinear algebraic equations for the positions of dislocations,

$$\frac{\gamma}{2\xi_i} + \sum_{j\neq i}^{N} \overline{\tau}^{b,j}(\xi_i) = 1, \quad (i = 1, 2, \cdots, N). \tag{10}$$

Following Öveçoğlu et al. (1987), we introduced in (10) the dimensionless coordinates

$$\xi_i = \frac{x_i}{\overline{x}}, \quad \overline{x} = \frac{k_1 b}{\tau^a}, \quad (i = 1, 2, \cdots, N), \tag{11}$$

and the dimensionless stresses are denoted by $\overline{\tau}^{b,j} = \tau^{b,j}/\tau^a$.

In the case of four selected values of φ, the incorporation of expressions (5)–(8) for $\tau^{b,\,j}(u_i)$ into (10) gives:

$$\varphi = 0°: \quad \sum_{j\neq i}^{N} \frac{1}{\xi_i - \xi_j} + \gamma \sum_{j=1}^{N} \frac{1}{\xi_i + \xi_j} + 2q \sum_{j=1}^{N} \frac{\xi_j(\xi_i - \xi_j)}{(\xi_i + \xi_j)^3} = 1, \quad (i = 1, 2, \cdots, N), \tag{12}$$

$$\varphi = 30°: \quad \sum_{j\neq i}^{N} \frac{1}{\xi_i - \xi_j} + \frac{\gamma}{2} \sum_{j=1}^{N} \frac{2\xi_i + \xi_j}{\xi_i^2 + \xi_j^2 + \xi_i\xi_j} + \frac{9q}{2} \sum_{j=1}^{N} \frac{\xi_i\xi_j^2\left(\xi_i^2 - \xi_j^2\right)}{\left(\xi_i^2 + \xi_j^2 + \xi_i\xi_j\right)^3} = 1, \tag{13}$$

$$\varphi = 45°: \quad \sum_{j\neq i}^{N} \frac{1}{\xi_i - \xi_j} + \gamma \sum_{j=1}^{N} \frac{\xi_i}{\xi_i^2 + \xi_j^2} - q \sum_{j=1}^{N} \frac{\xi_j\left(\xi_i^2 - \xi_j^2\right)\left(\xi_i^2 + \xi_j^2 - 4\xi_i\xi_j\right)}{\left(\xi_i^2 + \xi_j^2\right)^3} = 1, \tag{14}$$

$$\varphi = 60°: \quad \sum_{j\neq i}^{N} \frac{1}{\xi_i - \xi_j} + \frac{\gamma}{2} \sum_{j=1}^{N} \frac{2\xi_i - \xi_j}{\xi_i^2 + \xi_j^2 - \xi_i\xi_j} - \frac{q}{2} \sum_{j=1}^{N} \frac{\xi_j\left(\xi_i^2 - \xi_j^2\right)\left(2\xi_i^2 + 2\xi_j^2 - 5\xi_i\xi_j\right)}{\left(\xi_i^2 + \xi_j^2 - \xi_i\xi_j\right)^3} = 1. \tag{15}$$

Two dimensionless material parameters that appear in these expressions are q and γ, defined in terms of Dundurs parameters α and β by (2).

The system of nonlinear Eq. (10), and its special forms (12)–(15), were solved numerically by using the *fsolve* function within the Matlab software. Among three available iterative algorithms, *fsolve* chooses by default the trust-region dogleg algorithm based on the interior-reflective Newton method and the method of preconditioned conjugate gradients (Coleman and Li, 1994; Conn et al., 2000). Details of the numerical procedure based on an interior penalty function method, in which numerical solution is sought by solving a sequence of unconstrained minimization problems, can be found in Öveçoğlu et al. (1987).

Fig. 2a shows the equilibrium positions of $N = 5$ dislocations for different values of the shear moduli ratio $\Gamma = G_2/G_1 > 1$. The Poisson ratios are taken to be $\nu_1 = \nu_2 = 1/3$. The stiffer the interface (greater Γ), the stronger the repulsion exerted on dislocations and the more remote their positions from the interface. There is only a mild dependence of the overall dislocation distribution on the angle φ. Fig. 2b shows the same in the case of $N = 10$ dislocations. Due to stronger repulsion from other dislocations, the proximity of the leading dislocation to the interface increases with the increase of the number of dislocations in a pileup. Furthermore, for $N = 5$, the interface in a bimetallic solid repels the first and last dislocation in a glide plane with $\varphi \neq 0$ stronger than those in the glide plane with $\varphi = 0$. Depending on the number of dislocations in a pileup, several dislocations before the last dislocation can also be repelled stronger in the case $\varphi \neq 0$ than in the case $\varphi = 0$. For example, for $N = 10$ and the same set of considered material properties, the 1st, 9th, and 10th dislocations are repelled stronger; for $N = 15$, the 1st and the 12th–15th dislocations are repelled stronger; for $N = 20$, the first and the 16th–20th dislocations are repelled stronger. This is a consequence of the interplay of the contributions to the resolved-shear stress from individual dislocations in a pileup for differently inclined interface and the interface image effect on the dislocation stress fields. For a given N and φ, dislocations have to adjust their positions to make the total resolved shear stress along the glide plane, produced by dislocation interactions and remotely applied stress, vanish for each dislocation in its equilibrium position. The fact that the interface in a bimetallic solid repels the first and last dislocation in a glide plane with $\varphi \neq 0$ stronger than those in the glide plane with $\varphi = 0$ does not necessarily imply the same for all piled-up dislocations in-between.

The variation of ξ_1 with Γ is shown in Fig. 3a and c in the case of four selected values of the angle φ. Fig. 3b and d show the corresponding normalized length of the pileup $\xi_N - \xi_1$. Fig. 4 shows the variation of ξ_1 and $\xi_N - \xi_1$ with φ for pileups of 5 dislocations in the case $\Gamma = 2$, and $\nu_1 = \nu_2 = 1/3$. Similar plots can be obtained for other values of Γ. Both ξ_1 and $\xi_N - \xi_1$ increase with the increase of Γ. The effect of Poisson's ratios ν_1 and ν_2 on the dislocation distribution and the stress field can also be significant, which has been examined for orthogonal pileups by Öveçoğlu et al. (1987) and Lubarda (2017a).

4. Interface stresses

Piled-up dislocations cause large shear and tensile stresses at the interface between two materials, which can trigger slip on the other side of interface or nucleate cracks. The normal and shear stresses (σ_{uu}, σ_{uv}) along the interface, caused by dislocations, can be obtained by superposition of contributions from individual dislocations. From the general stress expressions listed in the Appendix, the dislocation-induced interface stresses, expressed in a dimensionless form $\hat{\sigma} = \sigma/\tau^a$ for each stress component, are

$$\hat{\sigma}_{uu}(0, \eta) = -\sum_{i=1}^{N} \frac{\eta c}{d_i^2}\left[g + (1 + q)\frac{3\xi_i^2 c^2 + (\eta - \xi_i s)^2}{d_i^2}\right] + 2sc \sum_{i=1}^{N} \frac{\xi_i}{d_i^2}, \tag{16}$$

$$\hat{\sigma}_{uv}(0, \eta) = \sum_{i=1}^{N} \frac{\xi_i - \eta s}{d_i^2}\left[g - (1 + q)\frac{\xi_i^2 c^2 - (\eta - \xi_i s)^2}{d_i^2}\right], \tag{17}$$

where $\xi_i = x_i/\overline{x}, \eta = v/\overline{x}, d_i^2 = \xi_i^2 c^2 + (\eta - \xi_i s)^2$, and $\overline{x} = k_1 b/\tau^a$. The abbreviations $c = \cos\varphi$ and $s = \sin\varphi$ are used. At the intersection of the interface and the glide plane, the stress components are

$$\hat{\sigma}_{uu}(0, 0) = \sin 2\varphi \sum_{i=1}^{N} \frac{1}{\xi_i}, \quad \hat{\sigma}_{uv}(0, 0) = [g - (1 + q)\cos 2\varphi] \sum_{i=1}^{N} \frac{1}{\xi_i}. \tag{18}$$

The interface stresses appearing in (16)–(18) depend on the material parameters g and $1 + q$, which are defined in (2).

Fig. 5a and b show the variation of the normalized stresses $\hat{\sigma}_{uu}$ and $\hat{\sigma}_{uv}$ along the interface in the case $N = 5, G_2/G_1 = 2$, and $\nu_1 = \nu_2 = 1/3$. Different curves correspond to four indicated values of the angle φ. Fig. 6a and b show the variation of the stress components $\hat{\sigma}_{uu}(0, 0)$ and $\hat{\sigma}_{uv}(0, 0)$ with $\varphi \in [0, 90°)$ at the point of the intersection of the glide plane and the interface in the case $N = 5$ and $\nu_1 = \nu_2 = 1/3$. Part (a) is for $G_2/G_1 = 2$ and part (b) for $G_2/G_1 = 4$. The magnitude of these stresses decreases with the increase of G_2/G_1 due to stronger repulsion exerted on dislocations by stiffer interface. While the shear stress

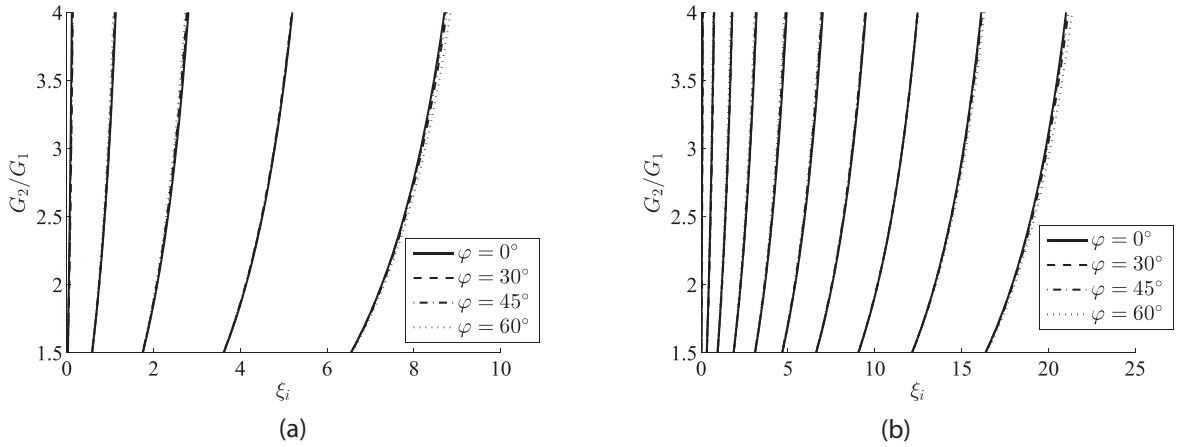

Fig. 2. (a) The equilibrium positions $\xi_i = x_i/\bar{x}$ of $N = 5$ dislocations vs. the shear moduli ratio $\Gamma = G_2/G_1$. The Poisson ratios are taken to be $\nu_1 = \nu_2 = 1/3$. The length scale is $\bar{x} = k_1 b/\tau^a$. (b) The same for $N = 10$ dislocations.

$\hat{\sigma}_{uv}(0, 0)$ is a monotonically increasing function of φ, the normal stress $\hat{\sigma}_{uu}(0, 0)$ has its maximum at $\varphi = 45°$. For larger N, the magnitude of interface stresses is significantly increased because dislocations are closer to the interface and there are more of them to build the stress.

5. Back stress behind a pileup

Piled-up dislocations exert a back stress behind a trailing dislocation of a pileup (ξ_N). This back stress opposes the resolved shear stress from the applied loading and may be sufficiently large to prevent further emission of dislocations from a dislocation source on a slip plane. This has the consequences on raising the flow stress of material and its rate of strain hardening (Hull and Bacon, 2011; Shetty, 2013). For a pileup in a homogeneous medium, with the leading dislocation pinned, the back stress along the glide plane, far behind a trailing dislocation ($x \gg x_N$), is $\tau^{\text{bs}} = NGb/[2\pi(1-\nu)x]$, where x is a distance from the pinned dislocation at $x = 0$ (Eshelby et al., 1951; Anderson et al., 2017). This stress variation is the same as the stress variation behind a superdislocation of the Burgers vector Nb, located at $x = 0$.

In the present context of the pileup against an inclined bimetallic

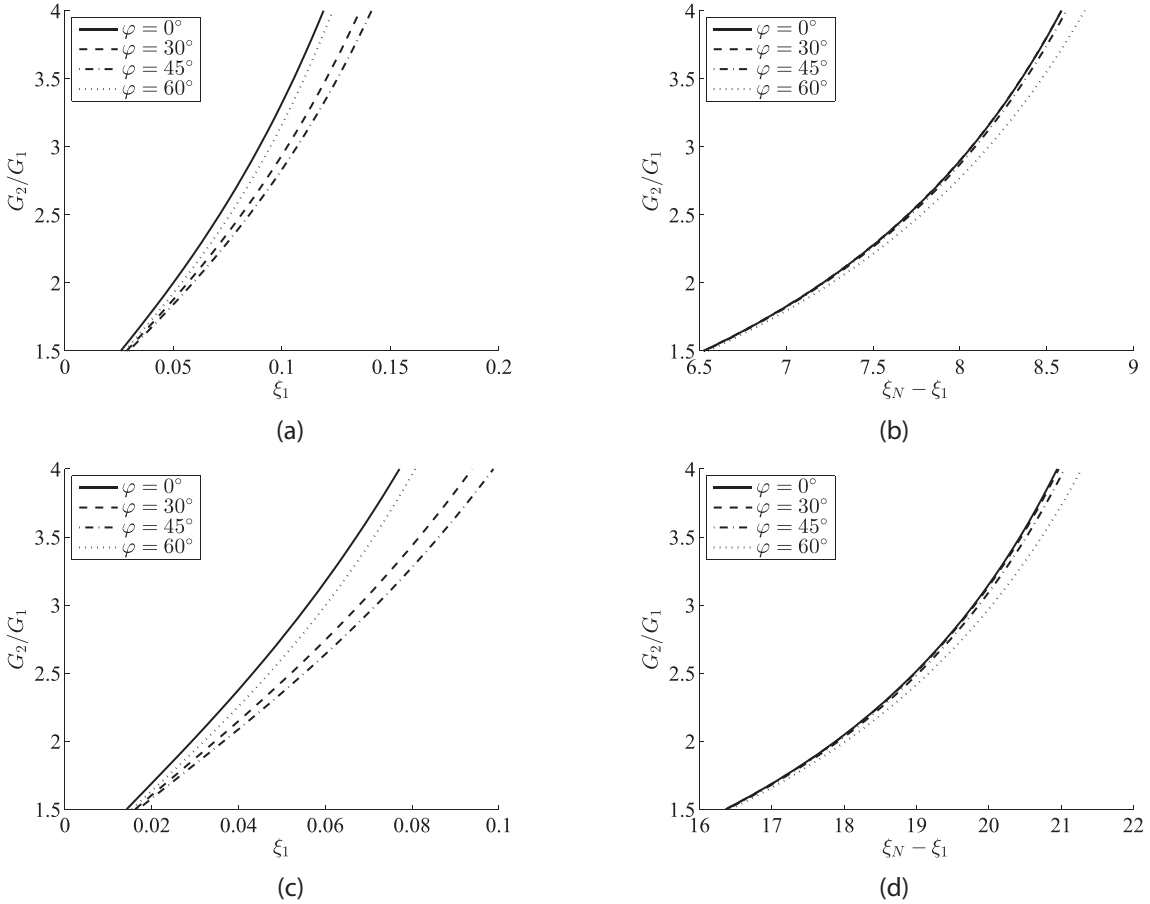

Fig. 3. (a) The position of the leading dislocation in the pileup ξ_1 vs. G_2/G_1 in the case $N = 5$ and $\nu_1 = \nu_2 = 1/3$. (b) The corresponding length of the pileup $(\xi_N - \xi_1)$. (c) & (d) The same as (a) and (b) in the case of $N = 10$ dislocations.

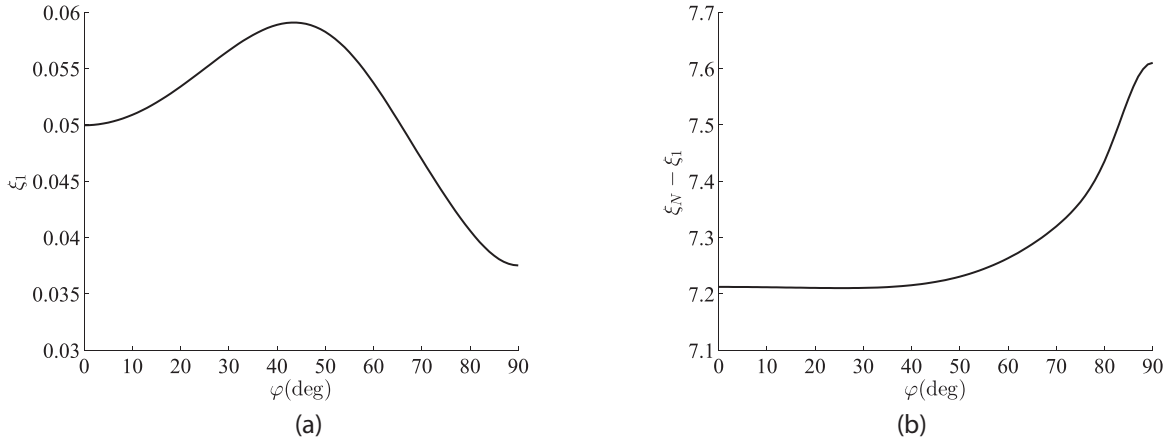

Fig. 4. (a) The position of the leading dislocation ξ_1 in the pileup of $N = 5$ dislocations vs. φ in the case $G_2/G_1 = 2$ and $\nu_1 = \nu_2 = 1/3$. (b) The corresponding length of the pileup $(\xi_N - \xi_1)$.

interface (Fig. 1), the back stress at any point $x > x_N$ along the glide direction, behind a trailing dislocation of the pileup (x_N), can be determined by summing-up the contributions from all dislocations in the pileup,

$$\tau^{\rm bs} = \sum_{i=1}^{N} \tau^i(x), \quad \tau^{b,i}(x) = -\frac{1}{2}(\sigma_{uu} - \sigma_{vv})^i(x)\sin 2\varphi + \sigma^i_{uv}(x)\cos 2\varphi, \tag{19}$$

where $(\sigma_{uu} - \sigma_{vv})^i(x)$ and $\sigma^i_{uv}(x)$ are specified by the expressions listed at the end of the Appendix of this paper. Fig. 7a shows the variation of the normalized back stress $\tau^{\rm bs}/\tau^a$ behind the trailing dislocation in the case of a pileup with $N = 5$,$\Gamma = G_2/G_1 = 2$, and $\nu_1 = \nu_2 = 1/3$. Two orientation angles ($\varphi = 0^\circ$ and 80°) are used, indicating a quite small effect of φ on the back stress. This is further illustrated in Fig. 7b, which shows the φ-variation of the back stress evaluated at the point $\xi = \xi_N + l$. The normalized length of the pileup is $l = L/\overline{x} = \xi_N - \xi_1$, where $\overline{x} = k_1 b/\tau^a$. Far behind a trailing dislocation ($\xi \gg l$), the back stress behaves as the stress behind a superdislocation of the Burgers vector Nb located at the interface, which is

$$\tau^{\rm sd} = k_1(1+\gamma)\frac{Nb}{x} = \tau^a(1+\gamma)\frac{N}{\xi}, \quad 1 + \gamma = \frac{1+\alpha}{1-\beta^2}. \tag{20}$$

The variation of $\tau^{\rm sd}/\tau^a$ is shown by a dotted curve in Fig. 7a.

6. Conclusions

Discrete pileups of edge dislocations against a flat bimetallic interface which is arbitrarily oriented relative to the pileup direction were considered. We solve numerically the nonlinear algebraic equations that specify equilibrium positions of dislocations, for a given number of dislocations and specified material properties. The magnitude of the resolved shear stress along the pileup direction was assumed to be uniform and equal for each inclination φ of the interface. The derivation of the expressions for the dislocation forces, which must vanish in equilibrium, is lengthy and tedious, but we were able to cast them in a relatively compact form for any angle φ. The simplified expressions were then deduced for $\varphi = 0^\circ$, 30°, 45°, and 60°. For a wide range of material parameters that were considered, the overall dislocation distribution was found to be mildly affected by the inclination of the interface, although there are some notable differences. While an inclined interface repels the first and last dislocation stronger than the interface orthogonal to the glide plane, for piled-up dislocations in-between this is not necessarily the case. Furthermore, small differences in the pileup length and the proximity of the leading dislocation to the differently oriented interface can considerably affect the interface stresses. The magnitude of these stresses decreases with the increase of the shear moduli ratio G_2/G_1 due to stronger repulsion exerted on dislocations by stiffer interfaces. The disparity in Poisson's ratio also affects the interface stresses. The variation of the back stress behind a trailing dislocation of a pileup is determined for different orientation of the interface. There is a small effect of φ on the magnitude of the back stress. Far behind a trailing dislocation, the back stress approaches the stress levels caused by a superdislocation of the Burgers vector Nb located at the interface, independently of φ. The presented analysis and the evaluated interface and back stresses may be of importance for the study of interface cracking, the onset of plastic yield, and the prediction of the rate of strain hardening in polycrystalline metal aggregates. Further mathematical analysis on whether the observations made in

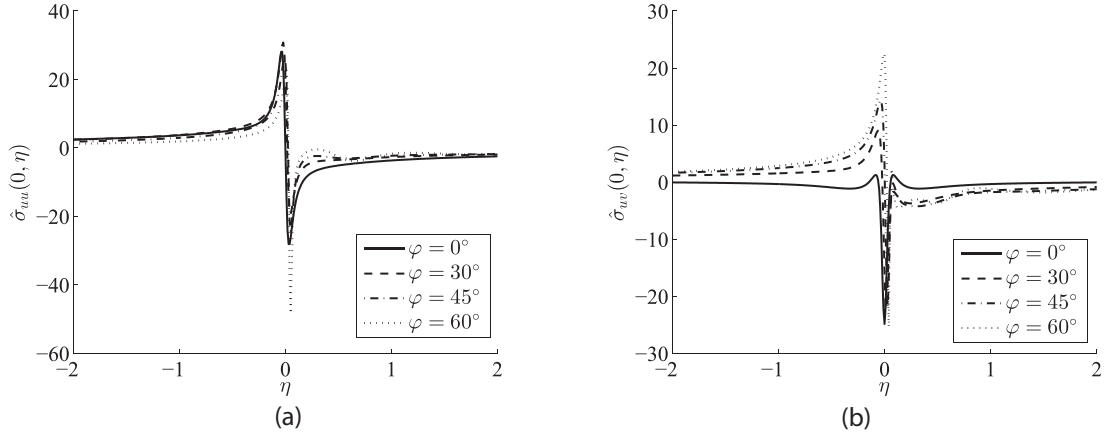

Fig. 5. a) The variation of $\hat{\sigma}_{uu}(0,\eta)$ along the interface in the case $N = 5$,$G_2/G_1 = 2$, and $\nu_1 = \nu_2 = 1/3$. (b) The same for the shear stress $\hat{\sigma}_{uv}(0,\eta)$.

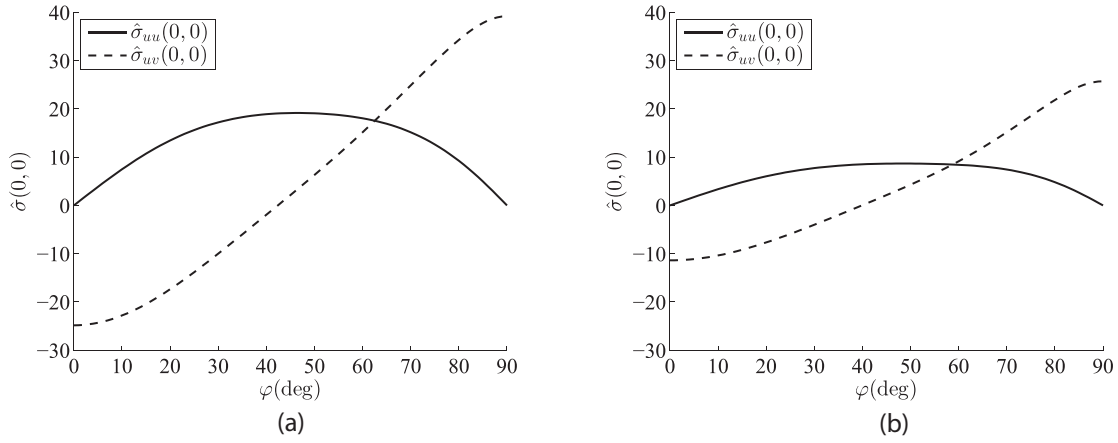

Fig. 6. The variation of the stress components $\hat{\sigma}_{uu}(0, 0)$ and $\hat{\sigma}_{uv}(0, 0)$ with φ for the pileup of $N = 5$ dislocations and Poisson's ratios $\nu_1 = \nu_2 = 1/3$, in the case: (a) $G_2/G_1 = 2$, and (b) $G_2/G_1 = 4$.

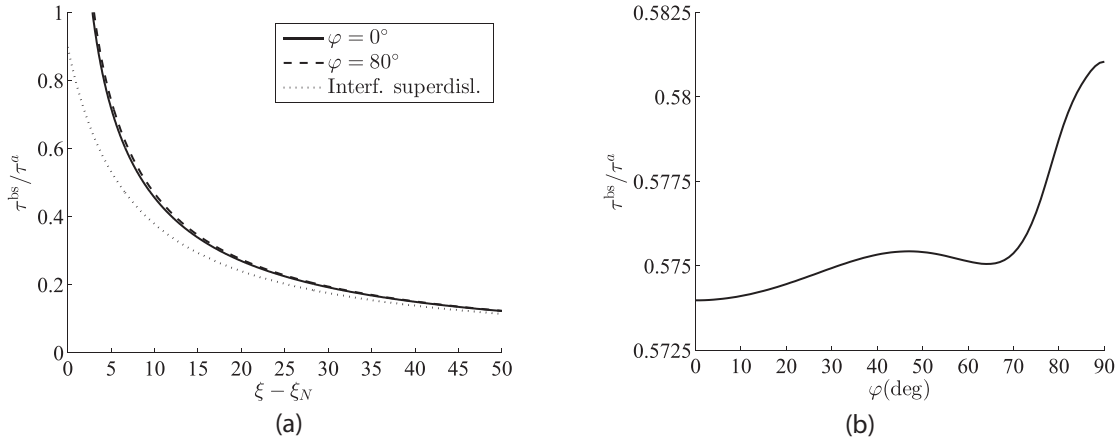

Fig. 7. (a) The variation of the back stress τ^{bs}/τ^a behind a trailing dislocation ξ_N in the case of a pileup with $N = 5$,$G_2/G_1 = 2$, and $\nu_1 = \nu_2 = 1/3$. (b) The variation of the back stress evaluated at $\xi = \xi_N + l$ with the orientation angle φ, where $l = \xi_N - \xi_1$ is the normalized length of the pileup. The pileup corresponds to $N = 5$,$G_2/G_1 = 2$, and $\nu_1 = \nu_2 = 1/3$.

this paper are true in the entire range of material parameters is a worthwhile goal of future investigation.

Acknowledgments

Research support from the Montenegrin Academy of Sciences and Arts is acknowledged. Discussions with Professor David M. Barnett from Stanford University are gratefully acknowledged. I also thank the two reviewers for their valuable comments and suggestions that greatly helped me to revise the manuscript.

Appendix A. Stresses from a dislocation near bimetallic interface

Referring to Fig. 8, and by using the expressions listed in Lubarda (1997) and Asaro and Lubarda (2006) for vertical interface, the stress components at an arbitrary point with coordinates (u, v), produced by the $b_u = b\cos\varphi$ component of an edge dislocation with a Burgers vector b, located at a distance x_i from the origin at O, along the indicated x direction, are

$$\sigma_{uu}^{b_u,i}(u,v) = -k_1 b_u (v - x_i s)\left[\frac{3(u + x_i c)^2 + (v - x_i s)^2}{r_i^4} + q\,\frac{3(u + x_i c)^2 + (v - x_i s)^2}{\rho_i^4} + 4qx_i cu\,\frac{3(u + x_i c)^2 - (v - x_i s)^2}{\rho_i^6} + g\,\frac{1}{\rho_i^2}\right],$$

$$\sigma_{vv}^{b_u,i}(u,v) = k_1 b_u (v - x_i s)\left[\frac{(u - x_i c)^2 - (v - x_i s)^2}{r_i^4} + q\,\frac{(u + x_i c)^2 - (v - x_i s)^2}{\rho_i^4} + g\,\frac{1}{\rho_i^2} + 4qx_i c\,\frac{(u + x_i c)^2(u - 2x_i c) - (3u + 2x_i c)(v - x_i s)^2}{\rho_i^6}\right],$$

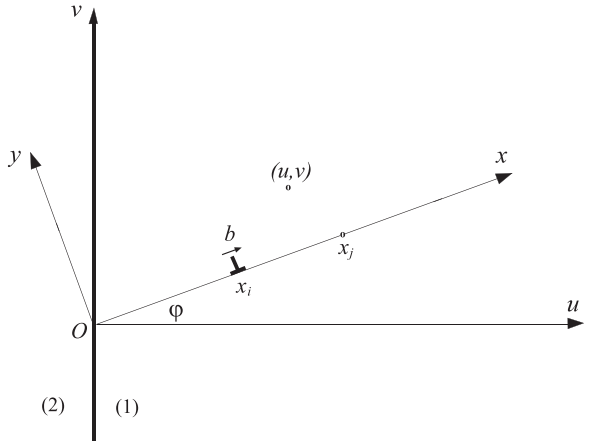

Fig. 8. An edge dislocation with a Burgers vector b at a distance x_i from a bimetallic interface. The angle between the glide direction (x) and the interface normal (u) is φ. The (u, v) components of the Burgers vector are $b_u = b\cos\varphi$ and $b_v = b\sin\varphi$. Indicated also is an arbitrary point with coordinates (u, v), and a point along the x-direction at a distance x_j from the origin at O.

$$\sigma_{uv}^{b_u,i}(u,v) = k_1 b_u \left\{ \frac{(u-x_i c)[(u-x_i c)^2-(v-x_i s)^2]}{r_i^4} + q\,\frac{(u+x_i c)[(u+x_i c)^2-(v-x_i s)^2]}{\rho_i^4} + 2qx_i c\,\frac{(u+x_i c)^3(u-x_i c)-6u(u+x_i c)(v-x_i s)^2+(v-x_i s)^4}{\rho_i^6} + g\,\frac{u+x_i c}{\rho_i^2}\right\}.$$

In these expressions, the parameters k_1, q, and g are defined by expressions (2) of Section 2, and the abbreviations are used $c = \cos\varphi$,$s = \sin\varphi$, and $r_i^2 = (u-x_i c)^2 + (v-x_i s)^2$, $\rho_i^2 = (u+x_i c)^2 + (v-x_i s)^2$.

Likewise, for the Burgers vector component $b_v = b\sin\varphi$, the stress components are

$$\sigma_{uu}^{b_v,i}(u,v) = k_1 b_v \left\{ \frac{(u-x_i c)[(u-x_i c)^2-(v-x_i s)^2]}{r_i^4} + q\,\frac{(u+x_i c)[(u+x_i c)^2-(v-x_i s)^2]}{\rho_i^4} - 2qx_i c\,\frac{(u+x_i c)^3(3u+x_i c)-6u(u+x_i c)(v-x_i s)^2-(v-x_i s)^4}{\rho_i^6} - g\,\frac{u+x_i c}{\rho_i^2}\right\},$$

$$\sigma_{vv}^{b_v,i}(u,v) = k_1 b_v \left\{ \frac{(u-x_i c)[(u-x_i c)^2+3(v-x_i s)^2]}{r_i^4} + q\,\frac{(u+x_i c)[(u+x_i c)^2+3(v-x_i s)^2]}{\rho_i^4} + 2qx_i c\,\frac{(u+x_i c)^3(u-x_i c)-6u(u+x_i c)(v-x_i s)^2+(v-x_i s)^4}{\rho_i^6} + g\,\frac{u+x_i c}{\rho_i^2}\right\},$$

$$\sigma_{uv}^{b_v,i}(u,v) = k_1 b_v \left\{ \frac{(v-x_i s)[(u-x_i c)^2-(v-x_i s)^2]}{r_i^4} + q\,\frac{(v-x_i s)[(u+x_i c)^2-(v-x_i s)^2]}{\rho_i^4} - 4qx_i cu(v-x_i s)\,\frac{3(u+x_i c)^2-(v-x_i s)^2}{\rho_i^6} - g\,\frac{v-x_i s}{\rho_i^2}\right\}.$$

The non-singular portions of these stresses at the center of the dislocation ($x = x_i$) are

$$\sigma_{uu}^{b,i}(x_i) = -\sigma_{vv}^{b,i}(x_i) = -k_1 b\,\frac{\gamma\tan\varphi}{2x_i}, \quad \sigma_{uv}^{b,i}(x_i) = k_1 b\,\frac{\gamma}{2x_i}, \quad (\varphi \neq 90^\circ).$$

The resolved shear stress along the u-direction is determined from the stress transformation formula $\tau = \sigma_{xy} = -(1/2)(\sigma_{uu}-\sigma_{vv})\sin 2\varphi + \sigma_{uv}\cos 2\varphi$, which gives

$$\tau^{b,i}(x_i) = k_1 b\,\frac{\gamma}{2x_i},$$

independently of φ ≠ 90°. This expression is used in Eq. (4) of Section 2.

At the point along the x-direction, at distance $x_j \neq x_i$ from the origin at O, the (u, v) coordinates are $(u, v) = x_j(c, s)$, while $r_i^2 = (x_j - x_i)^2$ and $\rho_i^2 = x_i^2 + x_j^2 + 2x_i x_j\cos 2\varphi$. Consequently, the previously listed stress expressions become

$$\sigma_{uu}^{b_u,i}(x_j) = -k_1 bsc(x_j-x_i)\left[\frac{1+2c^2}{(x_j-x_i)^2} + q\,\frac{3c^2(x_j+x_i)^2+s^2(x_j-x_i)^2}{\rho_i^4} + 4qc^2x_i x_j\,\frac{3c^2(x_j+x_i)^2-s^2(x_j-x_i)^2}{\rho_i^6} + g\,\frac{1}{\rho_i^2}\right],$$

$$\sigma_{vv}^{b_u,i}(x_j) = k_1 bsc(x_j - x_i)\left[\frac{c^2 - s^2}{(x_j - x_i)^2} + q\,\frac{c^2(x_j + x_i)^2 - s^2(x_j - x_i)^2}{\rho_i^4} + g\,\frac{1}{\rho_i^2} - 4qc^2x_i\,\frac{c^2(x_j + x_i)^2(2x_i - x_j) + s^2(x_j - x_i)^2(2x_i + 3x_j)}{\rho_i^6}\right],$$

$$\sigma_{uv}^{b_u,i}(x_j) = k_1 bc^2\left\{\frac{c^2 - s^2}{x_j - x_i} + q\,\frac{(x_j + x_i)[c^2(x_j + x_i)^2 - s^2(x_j - x_i)^2]}{\rho_i^4} + g\,\frac{x_j + x_i}{\rho_i^2} + 2qx_i(x_j - x_i)\,\frac{c^4(x_j + x_i)^3 - 6s^2c^2x_j(x_j^2 - x_i^2) + s^4(x_j - x_i)^3}{\rho_i^6}\right\},$$

and

$$\sigma_{uu}^{b_v,i}(x_j) = k_1 bsc\left[\frac{c^2 - s^2}{x_j - x_i} + q\,\frac{(x_j + x_i)[c^2(x_j + x_i)^2 - s^2(x_j - x_i)^2]}{\rho_i^4} - g\,\frac{x_j + x_i}{\rho_i^2} - 2qx_i\,\frac{c^4(x_j + x_i)^3(x_i + 3x_j) - 6s^2c^2x_j(x_j + x_i)(x_j - x_i)^2 - s^4(x_j - x_i)^4}{\rho_i^6}\right],$$

$$\sigma_{vv}^{b_v,i}(x_j) = k_1 bsc\left[\frac{1 + 2s^2}{x_j - x_i} + q\,\frac{(x_j + x_i)[c^2(x_j + x_i)^2 + 3s^2(x_j - x_i)^2]}{\rho_i^4} + g\,\frac{x_j + x_i}{\rho_i^2} + 2qx_i(x_j - x_i)\,\frac{c^4(x_j + x_i)^3 - 6s^2c^2x_j(x_j^2 - x_i^2) + s^4(x_j - x_i)^3}{\rho_i^6}\right],$$

$$\sigma_{uv}^{b_v,i}(x_j) = k_1 bs^2\left\{\frac{c^2 - s^2}{x_j - x_i} + q\,\frac{(x_j - x_i)[c^2(x_j + x_i)^2 - s^2(x_j - x_i)^2]}{\rho_i^4} - 4qc^2x_ix_j(x_j - x_i)\,\frac{3c^2(x_j + x_i)^2 - s^2(x_j - x_i)^2}{\rho_i^6} - g\,\frac{x_j - x_i}{\rho_i^2}\right\}.$$

The total stresses from both components of the Burgers vector are the sums of the corresponding expressions for the b_u and b_v component individually. For example, $\sigma_{uu}^{b,i}(x_j) = \sigma_{uu}^{b_u,i}(x_j) + \sigma_{uu}^{b_v,i}(x_j)$. The total resolved shear stress $\tau^{b,i}(x_j) = \sigma_{xy}^{b,i}(x_j)$ along the x-direction is then determined from

$$\tau^{b,i}(x_j) = -(\sigma_{uu} - \sigma_{vv})^{b,i}(x_j)sc + \sigma_{uv}^{b,i}(x_j)(c^2 - s^2),$$

where

$$(\sigma_{uu} - \sigma_{vv})^{b,i}(x_j) = -4k_1 bsc\left\{\frac{1}{x_j - x_i} + g\,\frac{x_j}{\rho_i^2} + q\,\frac{(x_j^2 - x_i^2)[c^2(x_j + x_i) + s^2(x_j - x_i)]}{\rho_i^4} + 2qc^2x_i\,\frac{c^2(x_j + x_i)^2(3x_j^2 - 2x_ix_j + x_i^2) - s^2(x_j - x_i)^2(5x_j^2 + 2x_ix_j - x_i^2)}{\rho_i^6}\right\},$$

$$\sigma_{uv}^{b,i}(x_j) = k_1 b\left\{\frac{c^2 - s^2}{x_j - x_i} + g\,\frac{c^2(x_j + x_i) - s^2(x_j - x_i)}{\rho_i^2} + q\,\frac{[c^2(x_j + x_i)^2 - s^2(x_j - x_i)^2][c^2(x_j + x_i) + s^2(x_j - x_i)]}{\rho_i^4} + 2qc^2x_i(x_j - x_i)\,\frac{c^4(x_j + x_i)^3 - 12s^2c^2x_j^2(x_j + x_i) + s^4(x_j - x_i)^2(3x_j - x_i)}{\rho_i^6}\right\}.$$

A1. Special cases

If the glide direction is orthogonal to the interface ($\varphi = 0°$), the resolved shear stress is

$$\tau^{b,i}(x_j) = k_1 b\left[\frac{1}{x_j - x_i} + \gamma\,\frac{1}{x_i + x_j} + 2q\,\frac{x_i(x_j - x_i)}{(x_i + x_j)^3}\right], \quad \gamma = q + g.$$

If the angle $\varphi = 30°$ angle, one obtains

$$\tau^{b,i}(x_j) = k_1 b\left[\frac{1}{x_j - x_i} + \frac{\gamma}{2}\,\frac{x_i + 2x_j}{x_i^2 + x_j^2 + x_ix_j} + \frac{9q}{2}\,\frac{x_i^2x_j(x_j^2 - x_i^2)}{(x_i^2 + x_j^2 + x_ix_j)^3}\right],$$

while for $\varphi = 45°$,

$$\tau^{b,i}(x_j) = k_1 b\left[\frac{1}{x_j - x_i} + \gamma\,\frac{x_j}{x_i^2 + x_j^2} - q\,\frac{x_i(x_j^2 - x_i^2)(x_i^2 + x_j^2 - 4x_ix_j)}{(x_i^2 + x_j^2)^3}\right].$$

Finally, if the glide direction is at $\varphi = 60°$, the resolved shear stress is

$$\tau^{b,i}(x_j) = k_1 b\left[\frac{1}{x_j - x_i} + \frac{\gamma}{2}\frac{2x_j - x_i}{x_i^2 + x_j^2 - x_i x_j} - \frac{q}{2}\frac{x_i(x_j^2 - x_i^2)(2x_i^2 + 2x_j^2 - 5x_i x_j)}{(x_i^2 + x_j^2 - x_i x_j)^3}\right].$$

A2. Back stress evaluation

The contributions to the back stress $\tau^{bs}(x)$ in Eq. (19) are obtained from the derived expressions in this appendix for $(\sigma_{uu} - \sigma_{vv})^{b,i}(x_j)$ and $\sigma_{uv}^{b,i}(x_j)$ by replacing in them x_j with x. This gives

$$(\sigma_{uu} - \sigma_{vv})^{b,i}(x) = -4k_1 bsc\left\{\frac{1}{x - x_i} + g\frac{x}{\rho_i^2} + q\frac{(x^2 - x_i^2)[c^2(x + x_i) + s^2(x - x_i)]}{\rho_i^4} + 2qc^2 x_i\frac{c^2(x + x_i)^2(3x^2 - 2xx_i + x_i^2) - s^2(x - x_i)^2(5x^2 + 2xx_i - x_i^2)}{\rho_i^6}\right\},$$

$$\sigma_{xy}^{b,i}(u) = k_1 b\left\{\frac{c^2 - s^2}{x - x_i} + g\frac{c^2(x + x_i) - s^2(x - x_i)}{\rho_i^2} + q\frac{[c^2(x + x_i)^2 - s^2(x - x_i)^2][c^2(x + x_i) + s^2(x - x_i)]}{\rho_i^4} + 2qc^2 x_i(x - x_i)\frac{c^4(x + x_i)^3 - 12s^2c^2x^2(x + x_i) + s^4(x - x_i)^2(3x - x_i)}{\rho_i^6}\right\},$$

with $\rho_i^2 = x^2 + x_i^2 + 2xx_i\cos 2\varphi$.

References

Anderson, P.M., Hirth, J.P., Lothe, J., 2017. Theory of Dislocations, Third ed. Cambridge Univ. Press, New York.

Asaro, R.J., Lubarda, V.A., 2006. Mechanics of Solids and Materials. Cambridge Univ. Press, Cambridge.

Barnett, D.M., 1967. The effect of shear modulus on the stress distribution produced by a planar array of screw dislocations near a bi-metallic interface. Acta Metall. 15, 589–594.

Barnett, D.M., Tetelman, A.S., 1967. The stresses produced by a screw dislocation pileup at a circular inclusion of finite rigidity. Can. J. Phys. 45, 841–863.

Baskaran, R., Akarapu, S., Mesarovic, S.D., Zbib, H.M., 2010. Energies and distributions of dislocations in stacked pile-ups. Int. J. Solids Struct. 47, 1144–1153.

Chou, Y.T., 1966. Equilibrium of linear dislocation arrays in heterogeneous materials. J. Appl. Phys. 37, 2425–2429.

Coleman, T.F., Li, Y., 1994. On the convergence of interior-reflective newton methods for nonlinear minimization subject to bounds. Math. Programm. 67, 189–224.

Conn, A.R., Gould, N.I.M., Toint, P.L., 2000. Trust Region Methods. MOS-SIAM Series on Optimization Society for Industrial and Applied Mathematics.

Dundurs, J., 1969. Elastic interactions of dislocations with inhomogeneities. In: Mura, T. (Ed.), Mathematical Theory of Dislocations. ASME, New York, pp. 70–115.

Eshelby, J.D., Frank, F.C., Nabarro, F.R.N., 1951. The equilibrium of linear arrays of dislocations. Phil. Mag. 42, 351–364.

Freund, L.B., 1993. The mechanics of dislocations in strained-layer semiconductor materials. In: Hutchinson, J.W., Wu, T.Y. (Eds.), Advances in Applied Mechanics. vol. 30. Academic Press, New York, pp. 1–66.

Geers, M.G.D., Peerlings, R.H.J., Peletier, M.A., Scardia, L., 2013. Asymptotic behaviour of a pile-up of infinite walls of edge dislocations. Arch. Ration. Mech. Anal. 209, 495–539.

Hall, C.L., 2010. Asymptotic expressions for the nearest and furthest dislocations in a pile-up against a grain boundary. Phil. Mag. 90, 3879–3890.

Head, A.K., 1953. Edge dislocations in inhomogeneous media. Proc. Phys. Soc. Lond. B66, 793–801.

Hull, D., Bacon, D.J., 2011. Introduction to Dislocations, Fifth ed. Butterworth-Heinemann. Elsevier, 2011.

Kapoor, R., Verdhan, N., 2017. Interaction of dislocation pile-up with a low-angle tilt boundary: a discrete dislocation dynamics study. Phil. Mag. A 97, 465–488.

Kuan, H., Hirth, J.P., 1976. Dislocation pileups near the interface of a bimaterial couple. Mater. Sci. Eng. 22, 113–131.

Kuang, J.G., Mura, T., 1968. Dislocation pile-up in two-phase materials. J. Appl. Phys. 39, 109–120.

Lubarda, V.A., 1997. Energy analysis of edge dislocation arrays near bimaterial interfaces. Int. J. Solids Struct. 34, 1053–1073.

Lubarda, V.A., 1998. Dislocation arrays at the interface between an epilayer and its substrate. Math. Mech. Solids 4, 411–431.

Lubarda, V.A., 2017. An analysis of edge dislocation pileups against a circular inhomogeneity or a bimetallic interface. Int. J. Solids Struct. In press.

Lubarda, V.A., 2017. A pileup of screw dislocations against an inclined bimetallic interface. Theor. Appl. Mech. 44. In press.

Lubarda, V.A., Kouris, D., 1996. Stress fields due to dislocation arrays at interfaces. Mech. Mater. 23, 191–203.

Öveçoğlu, M.L., Barnett, D.M., Nix, W.D., 1987. Analysis of the interfacial stresses produced by a pile-up of discrete edge dislocations in two phase materials. Acta Metall. 35, 1779–1789.

Scardia, L., Peerlings, R.H.J., Peletier, M.A., Geers, M.G.D., 2014. Mechanics of dislocation pile-ups: a unification of scaling regimes. J. Mech. Phys. Solids 70, 42–61.

Shetty, M.N., 2013. Dislocations and Mechanical Behaviour of Materials. PHI Learning, New Delhi.

Smith, E., 1972. The stress distribution near the tip of an array of screw dislocations piled-up against an inclusion. J. Mech. Phys. Solids 20, 307–312.

Thölén, A.R., 1970. The stress field of a pile-up of screw dislocations at a cylindrical inclusion. Acta Metall. 18, 445–455.

Voskoboinikov, R.E., Chapman, S.J., McLeod, J.B., Ockendon, J.R., 2009. Asymptotics of edge dislocation pile-up against a bimetallic interface. Math. Mech. Solids 14, 284–295.

Voskoboinikov, R.E., Chapman, S.J., Ockendon, J.R., 2007. Continuum and discrete models of dislocation pile-ups. II. pile-up of screw dislocations at the interface in a bimetallic solid. Phil Mag. Lett. 87, 669–676.

Wagoner, R.H., 1981. Calculating dislocation spacings in pile-ups at grain boundaries. Metall. Trans. A 12A, 2015–2023.

Zhang, X., 2017. A continuum model for dislocation pile-up problems. Acta Mater. 128, 428–439.